PROTEINS
STRUCTURE ■ FUNCTION ■ BIOINFORMATICS

Structural and functional analysis of substrate recognition by the 250s loop in amylomaltase from *Thermus brockianus*

Jong-Hyun Jung,[1†] Tae-Yang Jung,[2,3†] Dong-Ho Seo,[1] Sei-Mee Yoon,[2] Hyun-Chang Choi,[1] Byoung Chul Park,[2] Cheon-Seok Park,[1*] and Eui-Jeon Woo[2,3*]

[1] Graduate School of Biotechnology and Institute of Life Science and Resources, Kyung Hee University, Yongin 446-701, Korea

[2] Medical Proteomics Research Center, Korea Research Institute of Bioscience and Biotechnology, Daejeon 305-806, Korea

[3] Department of Bio-analytical Science, University of Science and Technology, Daejeon 305-333, Korea

ABSTRACT

Amylomaltase, or 4-α-glucanotransferase (EC 2.4.1.25), is involved in glycogen and maltooligosaccharide metabolism in microorganisms, catalyzing both the hydrolysis and transfer of an α-1,4-oligosacchraride to other sugar molecules. In this study, we determined the crystal structure of amylomaltase from *Thermus brockianus* at a resolution of 2.3 Å and conducted a biochemical study to understand the detailed mechanism for its activity. Careful comparison with previous amylomaltase structures showed a pattern of conformational flexibility in the 250s loop with higher B-factor. Amylomaltase from *T. brockianus* exhibited a high transglycosylation factor for glucose and a lower value for maltose. Mutation of Gln256 resulted in increased K_m for maltotriose and a sharp decrease of the transglycosylation factor for maltose, suggesting the involvement of Gln 256 in substrate binding between subsites +1 and +2. Mutation of Phe251 resulted in significantly lower glucose production but increased maltose production from maltopentose substrates, showing an altered substrate-binding affinity. The mutational data suggest the conformational flexibility of the loop may be involved in substrate binding in the GH77 family. Here, we present an action model of the 250s loop providing the molecular basis for the involvement of residues Phe251, Gln256, and Trp258 in the hydrolysis and transglycosylation activities in amylomaltase.

Proteins 2011; 79:633–644.

Key words: amylomaltase; 250s loop; substrate binding sites; *Thermus brockianus*.

INTRODUCTION

Starch is one of the most abundant natural polysaccharides and is an important energy resource. Because starch utilization is an essential pathway for growth, starch-converting enzymes are present in most microorganisms, plants, and animals.[1,2] Amylomaltase, or 4-α-glucanotransferase (EC 2.4.1.25), is one of the starch acting enzymes involved in glycogen and maltooligosaccharide metabolism in microorganisms. Amylomaltase catalyzes the biosynthesis of long chain maltooligosaccharides from short chain maltooligosaccharides.[3–5] A similar enzyme, known as the disproportionating enzyme (D-enzyme), exists in the starch metabolic pathway in plants.[6] D-enzyme and amylomaltase display significant homology in amino acid sequence[3] and have similar enzymatic properties: both enzymes catalyze the glucan transfer from one α-1,4-glucan to a new 4-position on an acceptor in glucose or another glucan (in a process termed disproportionation) and also synthesize varying lengths of cyclic α-1,4-glucans (in a process called cyclization). For example, the amylomaltase from *Thermus aquaticus* produces a cyclic α-1,4-glucan with a degree of polymerization (DP) of 22, whereas the potato D-enzyme produces a cyclic α-1,4-glucan with a DP of 17.[6,7] Both enzymes show hydrolysis and coupling activities that constitute the reverse reactions of disproportionation and cyclization. In the coupling reaction, cycloamylose is opened and transferred to an acceptor such as glucose by the enzyme. In the α-amylase reaction, hydrolysis occurs with water as an acceptor and amylose or cycloamylose is converted into linear short chain oligosaccharides.[8]

The amylomaltase family is classified into three groups, glycoside hydrolase (GH) families 13, 57, and 77.[9,10] Despite low levels of homology at the level of amino acid sequence, they share common catalytic properties. Generally, GH77 family amylomaltases are observed in many bacterial strains and some archaea.[11,12] The hyperthermophilic bacteria *Thermus aquaticus* and *Thermus thermophilus* amylomaltases, which have very high

Grant sponsor: National Research Foundation; Grant number: 2010-0011602; Grant sponsor: KRIBB Research Initiative Program
†These authors contributed equally.
*Correspondence to: Eui-Jeon Woo; E-mail: ejwoo@kribb.re.kr or Cheon-Seok Park; E-mail: cspark@khu.ac.kr.
Received 1 April 2010; Revised 20 August 2010; Accepted 25 August 2010
Published online 12 October 2010 in Wiley Online Library (wileyonlinelibrary.com).
DOI: 10.1002/prot.22911

homology with each other are the most studied GH77 enzymes. The three-dimensional structure of *T. aquaticus* amylomaltase revealed that it consists of catalytic domain A, TIM $(\beta/\alpha)_8$ barrel, and three inserted subdomains B1, B2, and B3.[3,13] The structure of amylomaltase from *T. aquaticus* in complex with acarbose showed that substrate binding sites −3 to +1 and secondary amylose binding sites around Tyr54 are important in cycloamylose formation.[13] From its crystal structure, amylomaltase was shown to have a structural fold and catalytic mechanism similar to the GH13 α-amylase family. Interestingly, the active site of α-amylase showed an open catalytic cleft, but amylomaltase has a flexible lid containing a long extended loop (250s loop) that partially covers the active site and forms part of the substrate binding site.[3,14] Cyclodextrin glucanotransferase (CGTase; EC 2.4.1.19) is a well-known GH13 family enzyme that produces cyclic α-1,4 glucans. Despite a lack of significant homology in their primary structures,[3,5] CGTase and amylomaltase catalyze similar reactions but produce cycloglucans of different sizes. Both CGTase and amylomaltase catalyze reactions including not only disproportionation and cyclization but also coupling and hydrolysis activity as side reactions.[8] Amylomaltase and CGTase are known to have higher transglycosylation activities compared with hydrolysis ability, and these activities are facilitated by hydrophobic interaction at the acceptor-binding site. Phe183 and Phe259 in CGTase from *Bacillus circulans* strain 251 are located in acceptor-binding site +2, which is involved in a hydrophobic interaction with the sugar ring of the substrate.[15] Mutation of these residues causes reduction of transglycosylation ability and results in α-amylase-like properties.[16]

GH77 family amylomaltases have a flexible lid containing the 250s loop located above the active site. Although the functional role of this loop has been proposed to be associated with substrate binding, neither its detailed role in substrate binding nor its involvement in the catalytic mechanism is fully understood. Recently, Kaper *et al.* reported that *T. thermophilus* amylomaltase has at least seven substrate binding sites in its active center.[14] They demonstrated that Asp249 in the 250s loop interacts with the substrate at the +2 acceptor-binding sites, and this binding affects the disproportionation reaction of the maltooligosaccharide. In a previous study, we isolated a thermostable amylomaltase from *T. brockianus* (TBGT) and studied some of its enzymatic properties. TBGT exhibits high sequence homology with the amylomaltases from *T. aquaticus* (86%), *T. thermophilus* (86%), and *T. scotoductus* (84%)[17] and displays high sequence conservation in the 250s loop when compared with other *Thermus* amylomaltases.

Here, we describe the crystal structure of TBGT and characterize the enzyme using activity assays on various substrates and acceptors. Based on the mutational study of Phe251, Gln256, and Trp258, we propose an action model of the flexible 250s loop during catalysis and provide the structural basis for the functional roles of these three residues in the hydrolysis and transglycosylation activities of the enzyme.

Table I
Data Collection and Structure Solution Parameters

Crystal type	Native
Unit cell parameters (Å)	a = 104.36, b = 104.36, c = 263.76
Resolution (Å)	29.93–2.36
Space group	$P6_522$
Completeness (%)	99.8 (96.0)
Average redundancy	21.4 (14.6)
R_{sym} (%)[b]	14.6 (49.6)
I/σ (I)	34.06 (5.36)
No. of refined atoms:protein/water	4045/110
R_{factor}/R_{free} (%)[c]	0.215/0.240
r.m.s.d. bond length (Å)	0.006
r.m.s.d. bond angle	1.2
Ramachandran plot (%)	
Most favored region	479 (96.8%)
Additionally allowed region	16 (3.2%)

[a]The numbers in parentheses are statistics from the highest resolution shell.
[b]$R_{sym} = \sum|I_{obs} - I_{avg}|/\sum I_{obs}$ where I_{obs} is the observed individual reflection and I_{avg} is the average over symmetry equivalents.
[c]R factor = $\sum||F_0|-|F_c||/\sum|F_0|$, where F_0 and F_c are the observed and calculated structure factor amplitudes, respectively. R_{free} was calculated using 5% of the data.

RESULTS

The flexible 250s loop

The crystal structure of TBGT was determined at a resolution of 2.3 Å by molecular replacement using the template structure of the amylomaltase from *T. thermophilus* (Table I).[18] The refined structure of the amylomaltase shows a configuration similar to the template, including a core domain of a $(\beta/\alpha)_8$ barrel and four subdomains (A, B1, B2, and B3) attached around the barrel [Fig. 1(A)]. The catalytic residues of Asp293 (nucleophile), Glu340 (general acid/base catalyst), and Asp395 (third catalytic residue) are well defined in the electron density map and show good overlapping alignment with template geometry [Fig. 1(C)].[3] The close proximity and the orientation of catalytic residues to subsite −1 indicate that TBGT would share the same catalytic mechanism with the retaining glucanotransferase-type amylomaltase from *T. thermophilus*.[18] There are flexible loops with notable variation in the regions of 242–261, 305–315, 341–346, and 464–472, which constitute the surrounding regions of the substrate binding sites [Fig. 1(B,E)].

In particular, the 250s loop constituting subsites −1 to +3 in the region of 247–255 exhibited a weak electron density and high conformational flexibility with an average B-factor of 65.7 compared with the average B-factor of 36.9 for the entire protein. Previously, this loop was shown to be involved in the substrate- and acceptor-binding activities of GH77 family enzymes.[3] Careful comparison of the loops in various amylase structures showed a regular pattern of the segmental flexibility of this motif suggesting that the conformational flexibility of this loop may be involved in binding substrates and regulating enzyme activity. For example, there is a significant positional difference of the loop between the structure in this study and the binary complex structure with an acceptor analog in

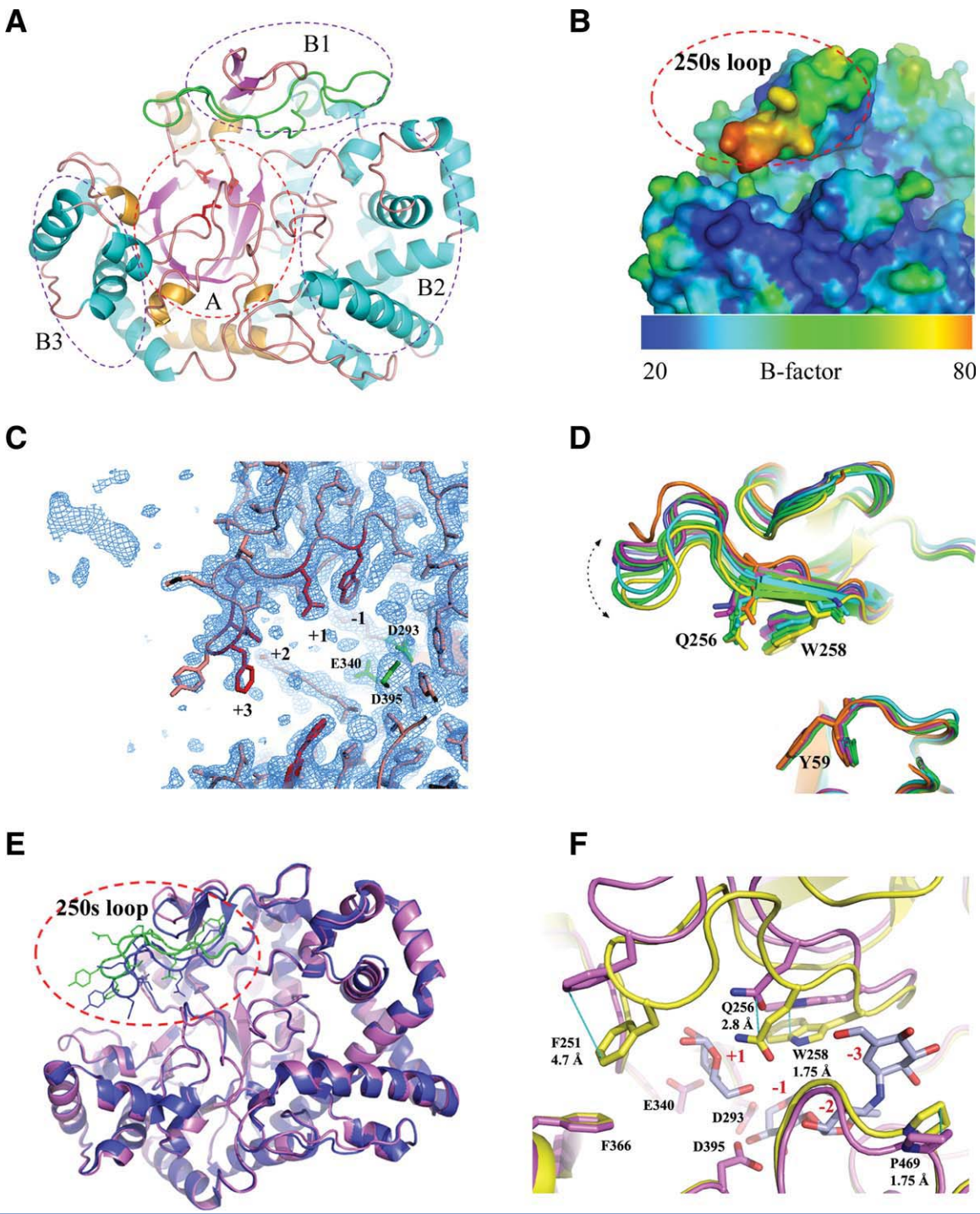

Figure 1

Overall Structure and the conformational flexibility of the 250s loop. (**A**) Schematic overview of TBGT with catalytic domain A and three subdomains B1, B2, and B3. The helix structure is shown in cyan with β-strands in magenta. The 250s loop is shown in green with the three catalytic residues (red stick). (**B**) Surface representation colored by B-factor. The color range bar represents the B-factor scale from 20 (blue) to 60 (orange) Å^2. (**C**) Electron density map of the 250s loop region. The substrate binding sites are shown for subsites −1 to +3 with catalytic residues colored in green. (**D**) Conformational flexibility of the 250s loop observed in superposition of TBGT (magenta) with various amylomaltase structures (PDB 1CWY, 1ESW, 1FP8, 1FP9, 1TZ7, 2OWC, 2OWW, 2OWX, 1X1N). The dotted arrow is shown to highlight the regular pattern of the segmental flexibility. (**E**) Superposition of TBGT with the amylomaltase structure from *T. thermophilus* (PDB 2OWW) with the surface colored by B-factor.[18] (**F**) Different conformation of the 250s loop in superposition of TBGT (magenta) with amylomaltase structure from *T. thermophilus* (yellow; PDB 2OWW). Movement of residues Trp258, Gln256, and Phe251 mutated in this study is indicated with the distance (cyan). The ligand molecule (4-deoxy-α-D-glucose and acarbose intermediate) at the active site is shown in light blue at subsites −3 to +1.

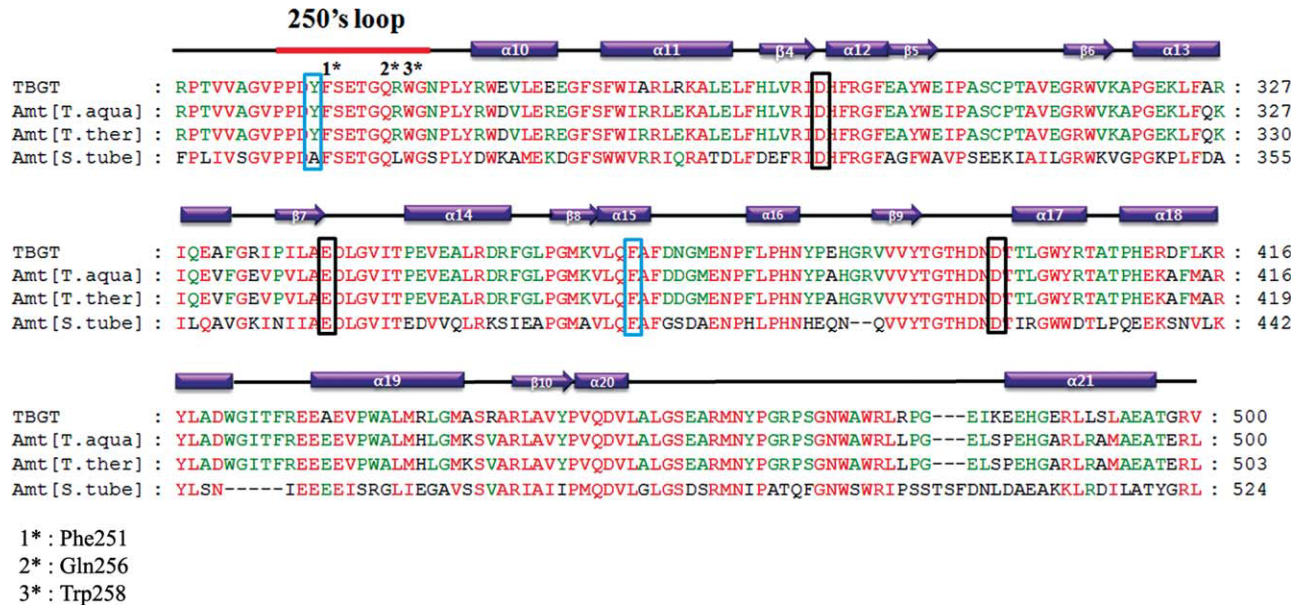

Figure 2

Sequence alignment of TBGT with other amylomaltases. Red, Green, and black colors represent residue groups conserved in 100, 75, and 50% of the proteins, respectively. Three conserved catalytic residues and the flexible 250s loop are boxed in black and blue, respectively. The putative substrate interacting residues are numbered from −1 to +3 according to the corresponding subsite position. The accession numbers for these sequences are AAY89060 (TBGT), BAA33728 (Amylomaltase from *Thermus thermophilus* [*T. ther*]), ZP_03497171 (Amylomaltase from *Thermus aquaticus* [*T. aqua*]), and Q06801 (D-enzyme from *Solanum tuberosum* [*S. tube*]).

the active site from *T. thermophilus*,[18] whereas the catalytic sites and the essential platform residue of Tyr59 at subsite −1 is completely superposed [Fig. 1(D,F)]. The different distances for residues Trp258, Gln256, and Phe251 between two structures are 1.75 Å, 2.53 Å, and 3.25 Å, respectively. For this reason, we chose these three residues on the 250s loop for mutation and conducted a biochemical study to further investigate the functional role of the loop and the possible involvement of conformational flexibility in the activity of amylomaltase (Fig. 2).

Characterization of TBGT

To investigate the enzymatic abilities of wild-type TBGT and its mutants, we measured amylose degradation activity and calculated the transglycosylation factor, because the transglycosylation factor indicates the transglycosylation ability of the enzyme with various acceptors.[19–21] Disproportionation activity was determined by measuring the rate of glucose released from various maltooligosaccharides (G3–G7) using HPAEC analysis.[14] The coupling/hydrolysis activities with cycloamylose and the cyclization/hydrolysis activities with amylose as the substrate were measured because these activities are good indicators of the relative transglycosylation activity.[19] Wild-type TBGT degraded amylose less efficiently (2.0×10 U/mg) compared with the degradation in the presence of acceptors such as glucose (1.1×10^3 U/mg) or maltose (5.7×10^3 U/mg) showing that amylomaltase requires acceptors to exhibit efficient amylose degradation (Table II). TBGT exhibited a twofold higher trans-

Table II

Amylose Degradation Activity and Transglycosylation Factors of WT and Mutant Enzymes for Acceptors of Glucose and Maltose

	Amylose degradation (U/mg)			Transglycosylation factor[a] (with acceptor/without acceptor)	
Enzyme	Glucose	Maltose	No acceptor	Glucose	Maltose
WT	$(1.1 \pm 0.2) \times 10^3$	$(5.7 \pm 0.2) \times 10^2$	$(2.0 \pm 0.1) \times 10^1$	$(5.4 \pm 0.6) \times 10^1$	$(2.8 \pm 0.2) \times 10^1$
F251G	7.1 ± 0.3	$(1.0 \pm 0.1) \times 10^1$	1.7 ± 0.0	4.1 ± 0.0	6.0 ± 0.2
Q256G	$(4.4 \pm 0.2) \times 10^1$	6.1 ± 0.2	0.8 ± 0.0	$(5.8 \pm 0.5) \times 10^1$	8.1 ± 0.7

[a]Transglycosylation factor was defined as the ratio of amylose degradation with acceptor relative to that without acceptor.

Table III
Enzyme Activity of WT and F251G Mutant for the Release of Glucose with G3-G7 Substrates

	F251		WT		
Substrate	Specific activity[a] (U/mg)	Ratio	Specific activity[a] (U/mg)	Ratio	Ratio WT/F251
G3	2.7 ± 0.3	1.0	(8.4 ± 0.7) × 10^4	1.0	(3.2 ± 0.3) × 10^4
G4	(4.9 ± 0.2) × 10^1	(1.9 ± 0.2) × 10^1	(8.1 ± 0.2) × 10^4	(9.7 ± 0.5) × 10^{-1}	(1.7 ± 0.0) × 10^3
G5	(1.0 ± 0.1) × 10^2	(3.9 ± 0.6) × 10^1	(7.1 ± 0.3) × 10^4	(8.5 ± 0.4) × 10^{-1}	(6.9 ± 0.8) × 10^2
G6	(9.3 ± 0.2) × 10^1	(3.5 ± 0.3) × 10^1	(5.0 ± 0.2) × 10^4	(6.0 ± 0.5) × 10^{-1}	(5.4 ± 0.3) × 10^2
G7	(4.7 ± 0.1) × 10^1	(1.8 ± 0.2) × 10^1	(1.7 ± 0.2) × 10^4	(2.1 ± 0.1) × 10^{-1}	(3.7 ± 0.4) × 10^2

[a]Specific activities for various maltooligosaccharides were determined by measuring the released glucose from the reaction with each 1 mM substrates, which was assayed by HPAEC analysis.

glycosylation factor with glucose than with maltose as the acceptor (transglycosylation factors of 5.4 × 10^1 and 2.8 × 10^1, respectively: Table II), suggesting that glucose is more efficient acceptor than maltose. The specific activity of WT for the disproportionation of G3 to G7 decreased with increasing maltooligosaccharide length (Table III). The disproportionation activity of WT with G3 as acceptor was twofold and sixfold higher than with G6 and G7, respectively, consistent with a previous report on the amylomaltase of *T. thermophilus*.[14] When maltopentaose was used as the substrate for the reaction, and the product was analyzed by HPAEC, TBGT produced glucose as the major product at a fourfold higher level than maltose (Fig. 3). The higher level of glucose in the reaction product with a high transglycosylation factor and the lower level of maltose with a low transglycosylation factor indicate that maltopentaose binds mainly at subsite −4 to +1 and subsite +2 has lower affinity to bind glucose moieties of the substrate at the reducing end, supporting the previously demonstrated substrate-binding properties of amylomaltase.[7,14]

Essential role of Trp258 in the hydrolysis activity of amylomaltase

The Trp258 residue is located in the 250s loop directly above substrate-binding subsite −1 in close proximity to the catalytic residues. This residue exists only in the amylomaltase family and not in other glycoside hydrolase or α-amylase families, and it has been suggested to be an important factor for the formation of cyclic products.[3] In the enzymatic assays of amylomaltase, the W258G mutant exhibited no hydrolysis activity of amylose and very low activity, if any, for the G3 substrate (2.5 U/mg; Tables II and IV). The W258G mutant showed neither cyclization nor coupling activity (Table VI), suggesting that residue Trp258 plays an essential role in all catalytic activities including hydrolysis and transglycosylation activities. The kinetic data with residual activity for maltotriose exhibited higher K_m values and lowered k_{cat} values, showing not only reduced substrate affinity to the binding site but also decreased catalytic efficiency (9.5 m*M* and 0.3 min^{-1}, respectively: Table V).

The role of Gln256 for acceptor binding at subsites +1 and +2

Gln256 was previously shown to be necessary for the correct orientation of an acceptor residue in the +1 subsite.[18] The Q256G mutant exhibited a trend similar to the wild type in disproportionation activity (data not shown). Although its production of glucose was lower than that of the wild type, maltotriose was the most suitable substrate among the maltooligosaccharides tested. Ratios of cyclization/hydrolysis and coupling/hydrolysis of the Q256G mutant were similar to those of wild-type TBGT (4.0 × 10^1 and 4.1, respectively; Table VI). The Q256G mutant had a significantly increased K_m value (165 m*M*) for the hydrolysis of maltotriose (Table V). Compared with the WT enzyme, a significant decrease in amylose degradation with glucose or maltose as the acceptor was detected for the Q256G mutant. Although amylose degradation was significantly reduced in the Q256G mutant, the transglycosylation factor of the mutant is similar to that of the WT enzyme (5.8 × 10^1 vs. 5.4 × 10^1; Table II). Notably, the decrease in amylose degradation activity was more severe for maltose as the acceptor than compared with that for glucose as the acceptor (1.1 × 10^3 to 4.4 × 10^1 U/mg for glucose and 5.7 × 10^2 to 6.1 U/mg for maltose) suggesting that incoming maltose molecules, which might occupy acceptor subsites +1 and +2, could not be suitably positioned in the Q256G mutant. Furthermore, the transglycosylation factor was much higher for maltose as the acceptor (2.8 × 10^1 to 8.1), whereas it was almost unchanged for glucose as the acceptor (5.4 × 10^1 to 5.8 × 10^1). This data strongly suggest that Gln256 is involved in substrate binding, in particular at subsite +2 in TBGT. Because this residue is known to bind O_5 and O_6 of the glucose molecule in the complex structure from *T. thermophilus*,[18] we believe that Gln256 may be involved in binding of the substrate linkage of two glucose moieties between subsites +1 and +2.

Alteration of the accepter binding in the F251G mutant

Phe251 is located at the tip of the flexible loop 16.8 Å from the catalytic residue of Asp293[3]. Mutational study

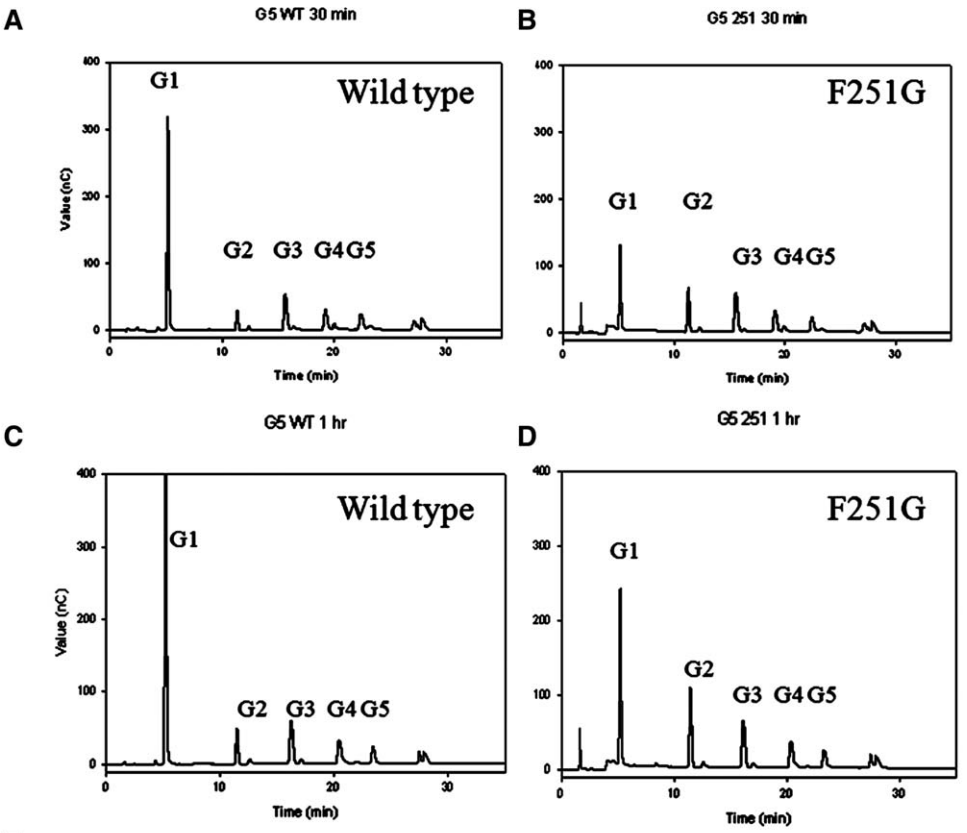

E

	WT			F251G		
Time (min)	Glucose (g/L)	Maltose (g/L)	Ratio (maltose/ glucose)	Glucose (g/L)	Maltose (g/L)	Ratio (maltose/ glucose)
10	0.29	0.07	**0.24**	0.05	0.10	**2.00**
30	0.37	0.12	**0.32**	0.14	0.28	**2.00**
60	0.51	0.20	**0.39**	0.26	0.52	**2.00**

Figure 3

HPAEC analysis of reaction products with maltopentose substrate and TBGT WT (left) and F251G mutant (right) after 30 min (**A,B**) and 60 min (**C,D**). The amount of the glucose and maltose products between TBGT wild type and the mutant F251G were compared (E).

showed that the F251G mutant exhibited a significant decrease of both hydrolysis and transferring activities. As shown in Table IV, the specific activity for maltotriose was reduced dramatically compared with that of wild type (2.7 U/mg vs. 8.4×10^4 U/mg) and the loss of activity in the F251G mutant was more severe than that of the Q256G mutant (ratio of 3.2×10^{-5} vs. 3.5×10^{-3}) despite Gln256s proximity to the active site. The F251G mutant displayed different substrate specificity in its disproportionation activity with higher affinity toward maltopenatose compared with other maltosaccharides (1.0×10^2; Table VI). Maltotriose and maltotetraose, relatively efficient substrates for the wild type, were less disproportionated by the mutation.

When maltopentaose was used as the substrate and the reaction product was analyzed by HPAEC, the F251G mutant showed significantly reduced production of glucose compared with the wild type (Fig. 3). The loss of transglycosylation activity in the presence of acceptor (glucose, 1.1×10^3 to 7.1 U/mg; maltose, 5.7×10^2 to 1.0×10^1 U/mg) was significantly greater than loss of the hydrolysis activity (2.0×10^1 to 1.7 U/mg) suggesting the involvement of this residue in the transglycosylation activity (Table II). The loss of cyclization (2.3×10^3 to 1.5 U/mg) for amylose or the loss of coupling activity (6.3×10^4 to 2.9×10^2 U/mg) for cycloamylose was higher than the loss of the hydrolysis activity for each substrate (Table VI). Additionally, the greater reduction

Table IV
Specific Activity of WT and TBGT Mutants F251, Q256, and W258 for Maltotriose and Amylose Substrates

Enzymes	Specific activity[a] (G3) (U/mg)	Ratio vs. WT	Specific activity[b] (amylose) (U/mg)	Ratio vs. WT
WT	$(8.4 \pm 0.7) \times 10^{4}$	1	$(2.0 \pm 0.1) \times 10^{1}$	1
F251G	2.7 ± 0.3	$(3.2 \pm 0.3) \times 10^{-5}$	1.7 ± 0.0	$(8.4 \pm 0.2) \times 10^{-2}$
Q256G	$(2.9 \pm 0.1) \times 10^{2}$	$(3.5 \pm 0.1) \times 10^{-3}$	0.8 ± 0.0	$(3.7 \pm 0.1) \times 10^{-2}$
W258G	2.5 ± 0.2	$(3.0 \pm 0.3) \times 10^{-5}$	ND[c]	–

[a]Specific activities for G3 was measured using the HPAEC analysis with 1 m*M* maltotriose.
[b]Specific activities for amylose was determined using the iodine assay with 0.4% amylase.
[c]Not determined.

of the ratios of coupling/hydrolysis and cyclization/hydrolysis compared with those of WT enzyme showed that the mutation affected the transglycosylation activity more severely.

The F251G mutant appeared to have significantly lost its glucose-binding affinity at subsite +1 because of the lower transglycosylation factor for glucose compared with the value for maltose (4.1 and 6.0, respectively: Table II) and the reduced disproportionation activity for G3 (2.7 U/mg; Table III). Consistent with these results, the F251G mutant yielded a much larger maltose product compared with the wild type indicating altered substrate-binding affinity (Fig. 3). Given the regular pattern of the flexibility observed in various crystal structures, we assume that the loss of affinity at subsite +1 and the increased binding affinity for maltose at subsite +1 and +2 were possibly caused by the conformational change of the 250s loop in the F251G mutant.

DISCUSSION

The 250s loop is highly conserved in GH77 family amylomaltases but is absent in GH13 and GH57 family amylomaltases.[3] The functional role of the 250s loop is of special interest in the GH77 family because of its architecture, whereby it forms a lid on the substrate-binding groove in subsites +1 to +3.[3,13,18] The flexibility of this extended loop observed in various crystal structures and the formation of substrate binding groove suggest that the segmental flexibility of the loop may be involved in substrate binding.[3,13,18] The range of the distance differences in Trp258, Gln256, and Phe251 between the current apo structure (2XLI) from *T. brockianus* and the binary structure complexed with an acceptor molecule (PDB 2OWW) from *T. thermophilus* becomes larger toward the tip of the lid, 1.75, 2.53, and 3.25 Å, respectively, with gradual increases, reminiscent of a hinge-like movement.[8] In fact, the possible involvement of this flexible loop in the substrate binding was previously suggested and the conformational change was proposed to be required for the catalytic activity.[3,14,18,22]

Here, we demonstrated the involvement of the loop in both hydrolysis and transglycosylation activities and provided the detailed enzymatic and biochemical data that acceptor binding was affected by mutation of the residues of the loop. Glucose was the most favored acceptor in the WT enzyme. Despite its significant distance from subsite +1, the reduced affinity for glucose in the F251G mutant can be explained by the inability of the 250s loop to adopt the proper conformation to bind the substrate for catalysis. The F251G mutant yielded a much larger maltose product than the WT enzyme using maltopentaose as a substrate, suggesting that the mutation caused altered substrate binding at the active site and resulted in a residual α-amylase property without transferring activity. Because Phe251 is close to Phe366 and is known to play a role in the hydrophobic stacking interaction with bound acceptor- or substrate,[3,19] the Phe251 mutant could not stabilize the extended loop any longer and possibly led to a promiscuous conformation of the lid, concomitantly allowing access to unfavorable acceptor such as maltose. For a characterization of the nature of the conformational change of the 250s loop, we utilized the domain motion analysis program "DynDom" (http://fizz.cmp.uea.ac.uk/dyndom/dyndomMain.do),[23] which determines regions moving as rigid bodies, hinge axes, and hinge-bending residues in proteins. When the current apo structure and the binary complex structure from *T. thermophilus* were analyzed, the program defined a moving domain, mainly the flexible 250s loop and part of the subdomain B1 (residues 146–149, 156–157, 215–221, 226–267, 272–274, 294–335: r.m.s.d 0.62 Å) and identified bending residues (residues 145–153, 155–158, 214–215, 221–222, 225–226, 267–280, 293–294, 335–338) with a hinge axis (rotation angle of 6.2°, translation along axis 0.3 Å), supporting our postulation [Fig. 4(A)].

Table V
Kinetic Parameters of WT TBGT and Its Mutant Enzymes for Maltotriose

Enzyme	K_m (m*M*)	k_{cat} (min^{-1})	k_{cat}/K_m (mM^{-1} min^{-1})
WT	2.0 ± 0.1	0.9 ± 0.1	$(4.2 \pm 0.5) \times 10^{-1}$
F251G	5.8 ± 1.0	0.1 ± 0.0	$(2.1 \pm 0.3) \times 10^{-2}$
Q256G	165 ± 15	4.8 ± 0.8	$(2.9 \pm 0.2) \times 10^{-2}$
W258G	9.5 ± 2.5	0.3 ± 0.1	$(2.9 \pm 0.1) \times 10^{-2}$

Table VI
Enzyme Activity of WT and Mutant Enzyme for Cyclization and Hydrolysis Activity with Amylose Substrate (left) and Coupling and Hydrolysis Activity with Cycloamylose Substrate (right)

	Amylose				Cycloamylose			
Enzymes	Cyclization activity (U/mg)	Hydrolysis activity (U/mg)	Cyclization/hydrolysis activity	Relative value	Coupling activity (U/mg)	Hydrolysis activity (U/mg)	Coupling/hydrolysis activity (103)	Relative value
WT	$(2.3 \pm 0.1) \times 10^{1}$	$(5.7 \pm 0.6) \times 10^{-1}$	$(4.0 \pm 0.6) \times 10^{1}$	1.0	$(6.3 \pm 0.5) \times 10^{4}$	$(1.2 \pm 0.1) \times 10$	5.2 ± 0.7	1.0
F251G	1.5 ± 0.2	$(5.1 \pm 0.3) \times 10^{-2}$	$(2.8 \pm 0.3) \times 10^{1}$	$(6.8 \pm 0.6) \times 10^{-1}$	$(2.9 \pm 0.4) \times 10^{2}$	$(3.0 \pm 0.1) \times 10^{-1}$	1.0 ± 0.3	$(1.9 \pm 0.5) \times 10^{-1}$
Q256G	1.6 ± 0.1	$(4.1 \pm 0.3) \times 10^{-2}$	$(4.0 \pm 0.3) \times 10^{1}$	$(9.5 \pm 0.9) \times 10^{-1}$	$(9.2 \pm 0.6) \times 10^{2}$	$(2.2 \pm 0.4) \times 10^{-1}$	4.1 ± 1.0	$(8.4 \pm 0.2) \times 10^{-1}$
W258G	ND[a]	ND[a]	–	–	$(1.4 \pm 0.1) \times 10$	ND*	–	–

[a]Not determined.

Thus, we propose that the segmental flexibility of the loop is an important property for amylomaltase in adopting an active state. Based on the mutational data and previous reports, we hypothesized an action model of the loop for the activity mechanism as drawn in Figure 4(B).[14,18,19] During transglycosylation and cyclization, residues Gln256 and Trp258 in amylomaltase may orient the substrate oligosaccharide in position at subsites −1 and +1 by moving downward in the loop, a similar functional role, respectively, corresponding to residues Phe183 and Tyr195 in CGTase, because Phe183 in CGTase from *Bacillus circulans* strain 251 is known to orient substrate molecules to subsite +1 in the acceptor-binding site, whereas Tyr195 cooperatively acts with Phe183 to guide linear substrates to the acceptor-binding site.[24] Trp258 moves downward at the active site pushing the glucose moiety to Tyr59 at subsite −1 to the correct position and allowing the scissile bond linkage of the substrate to adopt appropriate geometry for catalytic reaction by Asp293, Glu340, and Asp395. Cleavage of the scissile bond and formation of the covalent intermediate in the active site could adjust Trp258 to induce a conformational shift by a hinge-like motion, thereby removing the glucose from subsite +1. In the following step, an acceptor is required to bind in the narrowed subsite +1 for transglycosylation. When an acceptor molecule is bound to the acceptor-binding sites, the 250s loop would adjust the acceptor with residues Gln256 and Trp258 for proper positioning to catalyze the transglycosylation.

In summary, Trp258 is an essential residue for both hydrolysis and transglycosylation and Gln256 is necessary for the binding of acceptor molecules at subsites +1 and +2. Phe251 affects the substrate binding affinity at subsites +1 and +2 implicating the functional role of the 250s loop in the amylomaltase activity of GH77 family enzymes by utilizing the conformational flexibility of the loop.

MATERIALS AND METHODS

Reagents and enzymes

Maltooligosaccharides and cycloamylose (average MW: 7,500) were obtained from Wako Pure Chemical Industries (Osaka, Japan) and Ezaki Glico (Osaka, Japan), respectively. Potato amylose (type III) was purchased from Sigma-Aldrich (St. Louis, MO, USA). The synthetic oligonucleotides for mutagenesis were from Bionics (Seoul, Korea). *Escherichia coli* DH10B [F– *ara*D139 Δ(*ara leu*)7697 Δ*lac*X74 *gal*U *gal*K *rps*L *deo*R Φ80*lac*ZΔM15 *end*A1 *nup*G *rec*A1 *mcr*A Δ(*mrr hsdRMS mcrBC*)] and BL21(DE3) [F–, *omp*T, *hsd*S_B(r_B-, m_B-), *dcm*, *gal*, λ(DE3)] were used as hosts for cloning and expression, respectively. Expression vector pRSET-B (Invitrogen, Carlsbad, CA, USA) was used for the expression of wild-type amylomaltase from *T. brockianus* and its mutants. β-Amylase from *Bacillus cereus* that was

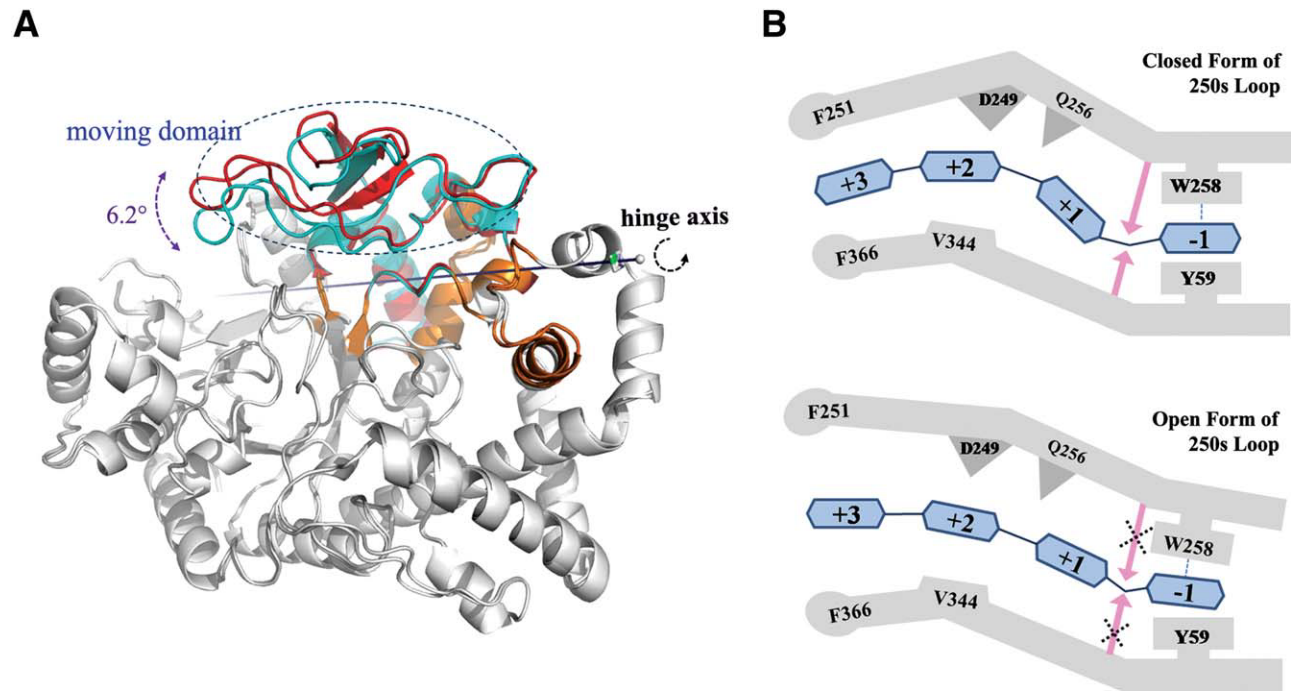

Figure 4

Possible action model of the flexible 250s loop. (**A**) Flexible moving domain between two amylomaltase structures (PDB 2XLI and 2OWW) analyzed by a program DynDom.[23] A fixed domain (white), a moving domain (red: 2XLI, cyan: 2OWW), bending residues (orange), and a hinge axis (black line) were defined with a rotation angle of 6.2° and a translation along the axis of 0.3 Å (Control parameters: window length 5, minimum ratio 1.0, minimum domain size 20). (**B**) A simplified model for the movement of the loop based on mutation data and structural analysis. The altered distance of Phe251 between the open and closed forms is highlighted by a blue line. An imaginary substrate is drawn as a light blue hexagon at subsites −1 to +3 based on the previous complex structure. The loss of the activity in open form is shown as a crossed pink arrow.

kindly provided by Dr. Kwan-Hwa Park in Incheon university was used for measurement of cyclization activity.

Site-directed mutagenesis (Construction of mutants, F251G and Q256G)

Site-directed mutagenesis was performed using a QuickChange kit (Stratagene, La Jolla, CA, USA). The *tbgt* gene in the pRSET-TBGT was used as template DNA for site-directed mutagenesis.[17] The synthetic oligonucleotides used as the primers for mutagenesis were constructed as follows: F251G: 5′-GTGCCCCCGGATTACGGCTCGG AAACCGGG-3′, Q256G: 5′-CTCGGAAACCGGGGGAC GCTGGGGCAAC-3′, and W258G: 5′-CCGGGCAACGC GGGGGCAACCCC-3′. The amplified PCR products were purified using a QIAquick Gel Extraction kit (Qiagen, Valencia, CA, USA) and transformed into DH10B and BL21(DE3). The sequence changes in the mutants were confirmed using the BigDye Terminator Cycle Sequencing Kit for ABI377 PRISM (Perkin–Elmer, Boston, MA, USA).

Purification of wild-type amylomaltase and its mutants

The *E. coli* BL21(DE3), which was transformed with plasmids harboring wild type or the mutated TBGT (pRSET-TBGT, pRSET-F251G, -Q256G, or -W258G), was grown at 37°C in LB medium containing 100 μg/mL ampicillin. When the optical density of the culture reached 0.6, the recombinant proteins were induced by the addition of 0.4 m*M* IPTG (isopropyl β-D-1-thiogalactopyranoside). After 3 h of induction at 37°C, the cells were harvested by centrifugation at 1,730*g* for 20 min at 4°C and washed with lysis buffer (pH 8.0; 50 m*M* NaH_2PO_4, 300 m*M* NaCl, and 10 m*M* imidazole). The cell pellets were disrupted by sonication (4 × 5 min, output control 4, 50% duty cycle; VC-600, Sonics & Materials, Newtown, CT, USA) and then heated at 60°C for 20 min. The cell debris and aggregated protein were eliminated by centrifugation at 15,610*g* for 30 min at 4°C. N-terminally six histidine-tagged enzymes were purified using nickel-nitrilotriacetic acid affinity column chromatography (Ni-NTA superflow™; Qiagen, Hilden, Germany). The supernatant was passed through an affinity column and washed with washing buffer (pH 8.0; 50 m*M* NaH_2PO_4, 300 m*M* NaCl, and 20 m*M* imidazole). The recombinant enzyme was eluted with elution buffer (pH 8.0; 50 m*M* NaH_2PO_4, 300 m*M* NaCl, and 250 m*M* imidazole). Protein concentrations were determined using the BCA method (Thermo Scientific, Rockford, IL, USA) with bovine serum albumin as the standard.

Crystallization and data collection

TBGT crystallization trials were conducted using the sitting drop method at 18°C. Protein solution of 1.5 μL (10 mg/mL) was mixed with equal volume of crystallization buffer containing 0.1*M* Bis-Tris (pH 6.5), 45% PPGP400, and 2.4% Inositol. Before data collection, crystals were cryo-cooled to 95 K using a cryoprotectant consisting of mother liquor supplemented with 25% glycerol. The crystal diffraction data was collected at the 4 A beamline of Pohang Accelerator Laboratory (PAL) at the wavelength of 1.000 (A).

Structure determination and refinement

Diffraction data were processed and scaled using HKL2000.[25] The structure was determined by the molecular replacement method using the Phaser CCP4 suite[26] with the structure of the 4-alpha-glucanotransferase (Protein Data Bank code 2OWC) as a search model. The result model was refined in conjunction with model rebuilding using CNS.[27] COOT[28] was used for stereographic manual refinement and model building. The structure was validated with PROCHECK.[29] Sequence alignments and structure-based sequence alignments were performed using ClustalW.[30] Molecular images, including cartoon and stick figures, were produced using Pymol.[31] Detailed statistics for the data collection and refinement is listed in Table I.

Enzyme activity assay

Disproportionation activity

The disproportionation activity of amylomaltase for various maltooligosaccharides was assayed by the glucose oxidase method.[12] A reaction mixture containing 10 m*M* maltooligosaccharides as substrate in 50 m*M* sodium citrate buffer (pH 6.0) was carried out at 70°C for 10 min. The reaction was stopped by adding 50 μL of 1*M* HCl. After neutralization with 50 μL of 1*M* NaOH, the reaction mixture was reacted with 900 μL of glucose oxidase solution at 37°C for 15 min to determine the concentration of glucose. The color developed was measured at 505 nm by spectrophotometer (Beckman DU 730, Fullerton, CA, USA). One unit of enzyme was defined as the amount of the enzyme that produces 1 nmol of glucose per min.

Coupling activity

To determine the coupling activity of amylomaltase, cycloamylose, and glucose were used as substrate and acceptor, respectively. A mixture containing 0.5% cycloamylose (w/v) and 10 m*M* glucose in 50 m*M* sodium citrate buffer (pH 6.0) was incubated at 70°C for 10 min. The coupling activity was assayed by measuring the reduction of the amount of glucose, as described above, using glucose oxidase. One unit of coupling activity was defined as the amount of enzyme that reduced 1 nmol of glucose per min.

Amylose degradation

Amylose degradation activity was determined by iodine method. A 100 μL reaction mixture containing 0.4% amylose dissolved in 90% dimethyl sulfoxide (DMSO) in 50 m*M* sodium citrate buffer (pH 6.0) was incubated at 70°C for 10 min. The reaction was stopped by addition of 50 μL of 1*M* HCl, and this was followed by neutralization with 1*M* NaOH. A 100 μL aliquot was mixed with 900 μL of Lugol's solution (0.2 g I_2 and 2.0 g KI in 1 L H_2O) at room temperature. The absorbance was measured at 660 nm and one unit of amylose degradation activity was defined as the amount of enzyme that hydrolyzed 1 mg of amylose per min. To measure amylose degradation activity in the presence of maltooligosaccharides as acceptors, 10 m*M* of acceptors were incubated with 0.4% amylose dissolved in 90% DMSO in 50 m*M* sodium citrate buffer (pH 6.0) at 70°C for 10 min. The transglycosylation factor was defined as the ratio of amylose degradation activity in the presence of acceptor relative to that in its absence.[19,21]

Cyclization activity

Cyclization activity was measured by monitoring the difference of the amount of reducing sugar produced by the β-amylase, which was treated to degrade linear maltooligosaccharides. β-Amylase from *Bacillus cereus* is unable to attack the cyclic glucans (cyclodextrins and cycloamyloses) due to the lack of a reducing end on the cyclic glucans.[20] A 100 μL reaction mixture containing 0.4% amylose dissolved in 90% DMSO in 50 m*M* sodium citrate buffer (pH 6.0) was incubated at 70°C for 2 h. The reaction was stopped by boiling for 20 min. The mixture was then treated with 0.24 U of β-amylase at 37°C for 10 h to degrade the remaining amylose into maltose. The reaction was terminated by adding DNS solution and boiled for 5 min. The absorbance was measured at 575 nm and one unit of cyclization activity was defined as the amount of enzyme that reduced 1 μmol of reducing sugar per min.

Hydrolysis activity

The measurement of reducing sugars by the DNS method was used to determine amylose and cycloamylose hydrolysis activity of amylomaltase. The reaction (500 μL) containing 50 μL of 4% amylose or cycloamylose as a substrate and 250 μL of 100 m*M* sodium citrate buffer (pH 6.0) were incubated at 70°C for 60 min. The reaction was terminated by adding DNS solution and boiled for 5 min. One units of hydrolysis activity was defined as

the amount of enzyme that produced reducing sugar equivalent to 1 μmol of maltose per min.

Determination of kinetic parameters

The kinetic parameters for the release of glucose were determined for WT TBGT and three mutant enzymes with various maltotriose substrate concentrations (1 to 10 m*M*). The assay was carried out at 70°C in 50 m*M* sodium citrate buffer (pH 6.0). The reaction mixtures were incubated for 100 min and the reaction samples were taken every 20 min before stopped by equal volume of 1*M* HCl. After neutralization with NaOH solution, the amount of glucose was measured by the glucose oxidase method. The kinetic parameters were determined using Lineweaver–Burk plots.

HPAEC analysis

High-performance anion exchange chromatography was performed using the DX-600 system (Dionex, Sunnyvale, CA, USA) with an ED50 electrochemical detector. A CarboPac^{TM} PA-100 column (0.4 × 25 cm, Dionex) was used to analyze the maltooligosaccharides, and buffer A (100 m*M* NaOH) and buffer B (100 m*M* NaOH in 500 m*M* sodium acetate) were used for elution at a flow rate of 1.0 mL/min. A multistep gradient was used for elution as follows: from 0 to 25 min, sodium acetate concentration was increased from 0 to 150 m*M*; from 25 to 26 min, increased from 150 to 500 m*M*; from 26 to 35 min, held at 500 m*M*; and from 35 to 40 min, decreased from 500 to 0 m*M*. Total 4 mU of WT or F251G mutant enzyme was added to the reaction buffer containing 50 m*M* sodium citrate buffer, pH 6, and 10 m*M* G5 substrate at 70°C.

Accession numbers

The atomic coordinates and structure factors (code 2XLI) have been deposited in the Protein Data Bank, Research Collaboratory for Structural Bioinformatics, Rutgers University, New Brunswick, NJ (http://www.rcsb.org/).

ACKNOWLEDGMENTS

The authors thank the staff at beamlines HFMX4A, Pohang Accelerator Laboratory, for data collection and technical assistance.

REFERENCES

1. Buchholz K, Seibel J. Industrial carbohydrate biotransformations. Carbohydr Res 2008;343:1966–1979.
2. MacGregor EA, Janecek S, Svensson B. Relationship of sequence and structure to specificity in the alpha-amylase family of enzymes. Biochim Biophys Acta 2001;1546:1–20.
3. Przylas I, Tomoo K, Terada Y, Takaha T, Fujii K, Saenger W, Strater N. Crystal structure of amylomaltase from *Thermus aquaticus*, a glycosyltransferase catalysing the production of large cyclic glucans. J Mol Biol 2000;296:873–886.
4. Dippel R, Boos W. The maltodextrin system of *Escherichia coli*: metabolism and transport. J Bacteriol 2005;187:8322–8331.
5. Takaha T, Smith SM. The functions of 4-α-glucanotransferases and their use for the production of cyclic glucans. Biotechnol Genet Eng Rev 1999;16:257–280.
6. Takaha T, Yanase M, Takata H, Okada S, Smith SM. Potato D-enzyme catalyzes the cyclization of amylose to produce cycloamylose, a novel cyclic glucan. J Biol Chem 1996;271:2902–2908.
7. Terada Y, Fujii K, Takaha T, Okada S. *Thermus aquaticus* ATCC 33923 amylomaltase gene cloning and expression and enzyme characterization: production of cycloamylose. Appl Environ Microbiol 1999;65:910–915.
8. van der Veen BA, van Alebeek GJ, Uitdehaag JC, Dijkstra BW, Dijkhuizen L. The three transglycosylation reactions catalyzed by cyclodextrin glycosyltransferase from *Bacillus circulans* (strain 251) proceed via different kinetic mechanisms. Eur J Biochem 2000;267:658–665.
9. Henrissat B. A classification of glycosyl hydrolases based on amino acid sequence similarities. Biochem J 1991;280(Pt 2):309–316.
10. Davies G, Henrissat B. Structures and mechanisms of glycosyl hydrolases. Structure 1995;3:853–859.
11. Godany A, Vidova B, Janecek S. The unique glycoside hydrolase family 77 amylomaltase from *Borrelia burgdorferi* with only catalytic triad conserved. FEMS Microbiol Lett 2008;284:84–91.
12. Kaper T, Talik B, Ettema TJ, Bos H, van der Maarel MJ, Dijkhuizen L. Amylomaltase of *Pyrobaculum aerophilum* IM2 produces thermoreversible starch gels. Appl Environ Microbiol 2005;71:5098–5106.
13. Przylas I, Terada Y, Fujii K, Takaha T, Saenger W, Strater N. X-ray structure of acarbose bound to amylomaltase from *Thermus aquaticus*. Implications for the synthesis of large cyclic glucans. Eur J Biochem 2000;267:6903–6913.
14. Kaper T, Leemhuis H, Uitdehaag JC, van der Veen BA, Dijkstra BW, van der Maarel MJ, Dijkhuizen L. Identification of acceptor substrate binding subsites +2 and +3 in the amylomaltase from *Thermus thermophilus* HB8. Biochemistry 2007;46:5261–5269.
15. van der Veen BA, Leemhuis H, Kralj S, Uitdehaag JC, Dijkstra BW, Dijkhuizen L. Hydrophobic amino acid residues in the acceptor binding site are main determinants for reaction mechanism and specificity of cyclodextrin-glycosyltransferase. J Biol Chem 2001;276:44557–44562.
16. Kelly RM, Leemhuis H, Dijkhuizen L. Conversion of a cyclodextrin glucanotransferase into an α-amylase: assessment of directed evolution strategies. Biochemistry 2007;46:11216–11222.
17. Bang BY, Kim HJ, Kim HY, Baik MY, Ahn SC, Kim CH, Park CS. Cloning and overexpression of 4-glucanotransferase from *Thermus brockianus* (TBGT) in *E. coli*. J Microbiol Biotechnol 2006;16:1809–1813.
18. Barends TR, Bultema JB, Kaper T, van der Maarel MJ, Dijkhuizen L, Dijkstra BW. Three-way stabilization of the covalent intermediate in amylomaltase, an α-amylase-like transglycosylase. J Biol Chem 2007;282:17242–17249.
19. Tang SY, Yang SJ, Cha H, Woo EJ, Park C, Park KH. Contribution of W229 to the transglycosylation activity of 4-α-glucanotransferase from *Pyrococcus furiosus*. Biochim Biophys Acta 2006;1764: 1633–1638.
20. Yang SJ, Min BC, Kim YW, Jang SM, Lee BH, Park KH. Changes in the catalytic properties of *Pyrococcus furiosus* thermostable amylase by mutagenesis of the substrate binding sites. Appl Environ Microbiol 2007;73:5607–5612.
21. Tachibana Y, Takaha T, Fujiwara S, Takagi M, Imanaka T. Acceptor specificity of 4-α-glucanotransferase from *Pyrococcus kodakaraensis* KOD1, and synthesis of cycloamylose. J Biosci Bioeng 2000;90:406–409.
22. Fujii K, Minagawa H, Terada Y, Takaha T, Kuriki T, Shimada J, Kaneko H. Function of second glucan binding site including tyrosines 54 and 101 in *Thermus aquaticus* amylomaltase. J Biosci Bioeng 2007;103:167–73.

23. Hayward S, Lee RA. Improvements in the analysis of domain motions in proteins from conformational change: DynDom version 1.50. J Mol Graph Model 2002;21:181–183.
24. Uitdehaag JC, van der Veen BA, Dijkhuizen L, Elber R, Dijkstra BW. Enzymatic circularization of a malto-octaose linear chain studied by stochastic reaction path calculations on cyclodextrin glycosyltransferase. Proteins 2001;43:327–335.
25. Otwinowski Z, Minor W. Processing of x-ray diffraction data collected in oscillation mode. Methods Enzymol 1997;276:306–326.
26. Collaborative Computational Project, Number 4. The CCP4 suite: Programs for protein crystallography. Acta Crystallogr Sect D Biol Crystallogr 1994;50:760–763.
27. Brunger AT, Adams PD, Clore GM, DeLano WL, Gros P, Grosse-Kunstleve RW, Jiang JS, Kuszewski J, Nilges M, Pannu NS, Read RJ, Rice LM, Simonson T, Warren GL. Crystallography and NMR system: a new software suite for macromolecular structure determination. Acta Crystallogr D Biol Crystallogr 1998;54:905–921.
28. Emsley P, Cowtan K. Coot: Model-building tools for molecular graphics. Acta Crystallogr D Biol Crystallogr 2004;60:2126–2132.
29. Laskowski RA, Moss DS, Thornton JM. Main-chain bond lengths and bond angles in protein structures. J Mol Biol 1993;231:1049–1067.
30. Thompson JD, Higgins DG, Gibson TJ. CLUSTAL W: Improving the sensitivity of progressive multiple sequence alignment through sequence weighting, position-specific gap penalties and weight matrix choice. Nucleic Acids Res 1994;22:4673–4680.
31. DeLano WL. Unraveling hot spots in binding interfaces: progress and challenges. Curr Opin Struct Biol 2002;12:14–20.